

## Tertiary Amide Rotation in a Nanoscale Host

Riccardo Salvio,<sup>[a][‡]</sup> Lionel Moisan,<sup>[a][‡]</sup> Dariush Ajami,<sup>[a]</sup> and Julius Rebek Jr.\*<sup>[a]</sup>**Keywords:** Molecular recognition / Encapsulation / Rotational barrier / Self-assembly / Coalescence method

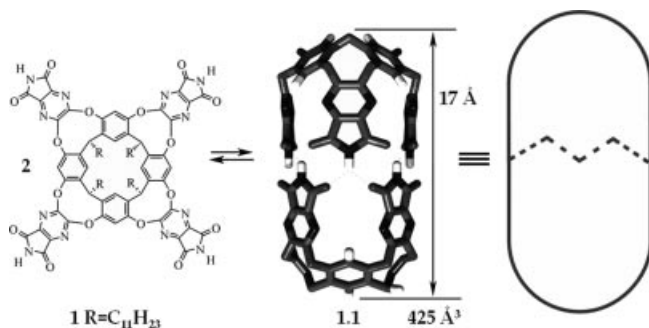
A self-assembled cylindrical capsule provides a nanoscale environment that affects the rotational barriers of tertiary amides. Measurements of the activation energies for the rotations and behaviors of the amides inside the capsule were determined by using  $^1\text{H}$  NMR spectroscopic methods in deuterated mesitylene solution. For amides **3–8**, rotation rates can decrease or increase in the capsule by up to an order of magnitude from those of the free amides in solution depending on the structure of the amides. The acceleration/deceleration of the rotation results from selective destabiliza-

tion/stabilization of the ground state or the transition state. In the case of compound **10**, the rotation generates two isomers that are equimolar in solution but inside the capsule only one of them is observed. Accordingly, the rotation rate is slowed by several orders of magnitude inside the capsule. In the case of amide **8**, a competition experiment indicates that the acceleration of the rotation inside the capsule is due to destabilization of the ground state.

(© Wiley-VCH Verlag GmbH & Co. KGaA, 69451 Weinheim, Germany, 2007)

## Introduction

Cylindrical cavitand **1** is known to form dimers by hydrogen bonding to create a host for a variety of guest molecules inside.<sup>[1]</sup> Dimer **1·1** provides a well-defined environment in which the guests are able to interact with each other and the inner walls of the capsule at a close distance. These interactions are able to affect the conformation and/or the molecular motions of the encapsulated molecule.<sup>[1b,1c]</sup> In addition, energy barriers for the rotation about the bonds of the guest can, at least in principle, be changed as a result of the attractive or repulsive interactions taking place within the cavity of the host.



Earlier investigations revealed that the molecular motion of a guest inside the capsule can be manipulated. It was

shown that the rotation rate of a cyclophane along the axis of **1·1** can be controlled and tuned by varying the size of the coguest;<sup>[2]</sup> Sherman et al. studied the rotation of pyrazine along an axis of a carceplex.<sup>[3]</sup> Encapsulation can also affect the internal molecular motions of a molecule. Ring inversion of cyclohexane hosted in a different capsule was studied, but only a small effect on the inversion rate of the cyclohexane ring was observed.<sup>[4]</sup>

In the present study we investigate the rotational barriers of encapsulated tertiary amides and compare them with the barriers of the free molecules in solution.

The *cis-trans* isomerization of tertiary amides is an extensively investigated phenomenon and studies of the rates of this isomerization have been reported in the literature for numerous amides.<sup>[5,6]</sup> The energy barrier for rotation of the C–N bond is relatively high compared to the barriers about other covalent bonds. This is due to the partial  $\pi$ -bond character between the carbonyl group and the nitrogen atom that forces the amide function to be planar. The energy barrier is high enough to study this phenomenon by NMR spectrometry around room temperature. It is also known that the rotation rate of amides is affected by the solvent and by the interaction of the oxygen of the carbonyl group with Lewis acids;<sup>[6,7]</sup> we therefore examined the rotation of amides in a fixed solvent, which also provides the surrounding environment in capsule **1·1**.

The behavior of *N,N*-dimethylacetamide (DMA) and *N,N*-dimethylformamide (DMF) has been studied in a carceplex;<sup>[8]</sup> the rotation of DMA was slowed inside the carceplex whereas the rotation of DMF was accelerated. This led Cram to propose that the carceplex was a different phase, but it is now generally accepted that reversible encapsulation complexes are quite like the liquid phase.

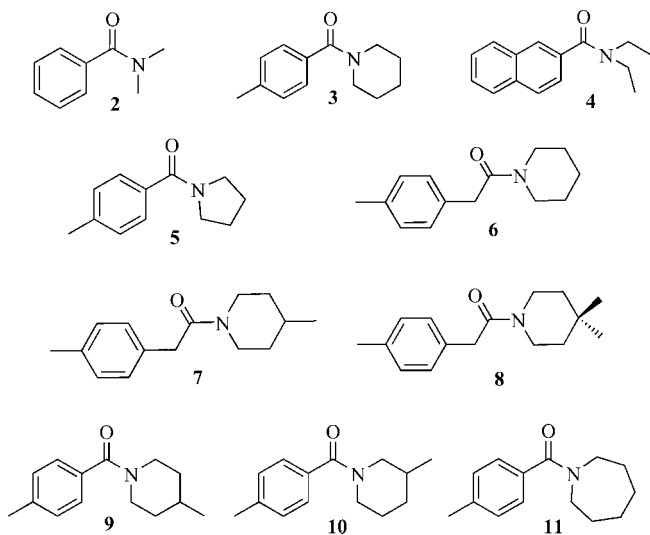
[a] The Skaggs Institute for Chemical Biology, The Scripps Research Institute, Mail MB-26, 10550 North Torrey Pines Road, La Jolla, CA 92037 USA, Fax: +1-858-784-2876, E-mail: jrebek@scripps.edu

[‡] Both authors contributed equally to this work.

Supporting information for this article is available on the WWW under <http://www.eurjoc.org> or from the author.

The study of the effects of a defined cavity on the rotational barriers also has biorelevance because Nature provides nanoscale cavities in enzymes in which the rotational barrier for the isomerization of proline is altered. These enzymes are able to catalyze the rotation of proline about the C–N bond by different mechanisms.<sup>[9]</sup> The *cis*–*trans* isomerization of peptidylproline plays a crucial role in the conformational changes of proteins; for this reason proline can be compared to a molecular switch.<sup>[10]</sup> Peptidylprolyl *cis*–*trans* isomerase (PPIase) was the first enzyme found to catalyze this conformational interconversion.<sup>[11]</sup> At least three families of such enzymes are now known: cyclophilins, FK506 binding protein, and parvulins.<sup>[12]</sup>

In the present work we studied the rotational barriers of tertiary amides **2**–**11** encapsulated in dimer **1**·**1**.



## Results and Discussion

For such a study, the guests must form stable encapsulation complexes in a temperature range that is wide enough for the measurements to be made and show NMR signals that undergo coalescence phenomena that do not overlap with the signals of the capsule or the free guest. For these reasons, we synthesized amides **3**–**11** that were likely, because of their size and shape, to be good guests.<sup>[13]</sup> These amides have aliphatic protons that, when encapsulated, give signals in the far upfield region of the <sup>1</sup>H NMR spectrum. We acquired 1D and, when necessary, 2D <sup>1</sup>H NMR spectra of these guests in the presence of **1** in deuterated mesitylene solution.

We assigned the signals of the encapsulated amide and studied the changes in the spectra with temperature to evaluate the energy barriers of the rotation about the C–N bond. Mesitylene was chosen as the solvent because it does not fit into the cavity of **1**·**1**, and therefore it does not compete with the amides for encapsulation.<sup>[14]</sup> For a homogeneous comparison, mesitylene was also used to study the barrier of the free guests in solution because this solvent closely resembles the aromatic walls of the capsule. Ad-

ditionally, the capsule can be thought of as an environment in which the solvent is preorganized and fixed in the space.

We determined the rate constants of this rotation for most of the guests. In some cases, the complexity of the spectrum and/or the instability of the capsule did not allow an estimate of the energy barriers. Initially, a line-shape analysis approach was tried. The shape of the peaks involved in the chemical exchange is mathematically described by an equation derived from the Bloch equations.<sup>[15]</sup> With this method, and fitting the spectrum with the calculated one, it is possible to determine the rate constants for the rotation at different temperatures. By fitting all the experimental data using Eyring theory [see Equation (1)], the values of  $\Delta H^\ddagger$  and  $\Delta S^\ddagger$  for the rotation about the C–N bond were obtained. The rate constants measured with this method show linear Arrhenius plots but unfortunately these figures turned out to be affected by large systematic errors as previously reported in the literature.<sup>[16]</sup> The values of the activation parameters obtained from these measurements were very different for the amides investigated, but the values of  $\Delta G^\ddagger$  were close to each other for different guests, probably because of error compensations. The absolute values of  $\Delta S^\ddagger$  for the rotation of many guests were very high, whereas for rotation about a bond, the activation entropy is expected to be very close to zero. Therefore, we decided to use the coalescence method, which is the most common and accepted method in the literature, to evaluate these energy barriers. According to this method, when two signals are in chemical exchange, it is possible to obtain the rate constant of the process at the coalescence temperature by Equation (2), where  $\nu_a$  and  $\nu_b$  are the frequencies of the peaks at the slow exchange limit.<sup>[15]</sup>

$$k = \frac{K_b T}{h} e^{\frac{\Delta G^\ddagger}{RT}} = \frac{K_b T}{h} e^{\frac{\Delta H^\ddagger - T\Delta S^\ddagger}{RT}} \quad (1)$$

$$k_{T_c} = \frac{\pi(\nu_a - \nu_b)}{2} \quad (2)$$

From the rate constant at the coalescence temperature, it is possible to obtain the rotational energy barrier by the Eyring equation [Equation (1)]. The value of this barrier is  $\Delta G^\ddagger$ , but if we assume, according to the arguments above, that  $\Delta S^\ddagger$  is close to zero and therefore negligible, this barrier can be considered as the enthalpy of activation. For this reason, it is acceptable to compare the energy barriers even if they are measured at different temperatures. The coalescence method provided measurements accurate enough for the purposes of this study. Table 1 reports the values of these barriers for amides **3**–**8**. For the other guests, it was not possible to obtain a quantitative estimate of the barriers. Guest **2**, for example, was encapsulated only in the presence of CH<sub>2</sub>Cl<sub>2</sub> as a coguest. Unfortunately, it was not such a good guest for **1**·**1** and the methyl signals were not shifted upfield enough to study the coalescence of the peaks.<sup>[17]</sup>

In contrast, amide **3** forms a very stable complex in **1**·**1**. Well-defined signals appear in the upfield region of the  $^1\text{H}$  NMR spectrum (see Figure 1).

Table 1. Energy barriers<sup>[a]</sup> [kcal mol<sup>-1</sup>] for the rotation of amides **3**–**8** inside dimer **1**·**1** and in mesitylene solution.

Amide	$\Delta G^{\ddagger}_{\text{out}}$ <sup>[b]</sup>	$\Delta G^{\ddagger}_{\text{in}}$ <sup>[b]</sup>	$\Delta G^{\ddagger}_{\text{in}} - \Delta G^{\ddagger}_{\text{out}}$	$k_{\text{in}}/k_{\text{out}}$ <sup>[c]</sup>
3	13.2	14.4	1.2	0.13
4	13.4	14.8	1.4	0.10
5	14.6	14.4	-0.2	1.4
6	15.4	15.1	-0.3	1.7
7	15.2	15.2	0.0	1.0
8	15.6	14.2	-1.4	10.7

[a] Coalescence method measurements [Equation (2)], 600 MHz; error limit  $\leq 0.2$  kcal mol<sup>-1</sup>. [b] Calculated by Eyring theory [Equation (1)]. [c] Calculated at 300 K.

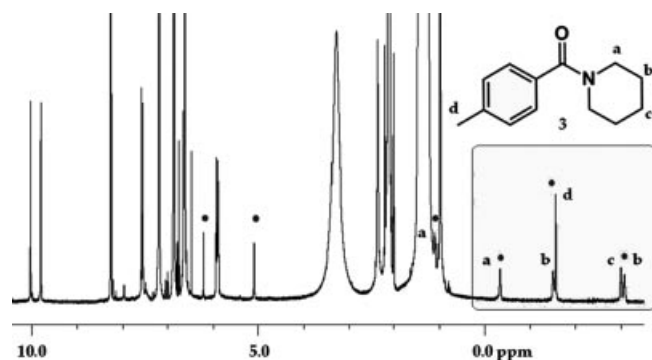


Figure 1. 600 MHz  $^1\text{H}$  NMR spectrum of amide **3** at 300 K encapsulated in **1**·**1** in deuterated mesitylene; (•) signals of the encapsulated guest.

The  $^1\text{H}$  NMR spectrum of **3** in deuterated mesitylene at 300 K shows that the  $\alpha$  methylene protons (and the  $\beta$  methylene protons) of the piperidine ring are in fast exchange on the NMR timescale.<sup>[17]</sup> Inside the capsule, the rotation seems to be frozen. The COSY  $^1\text{H}$  NMR spectrum of **3** encapsulated in **1**·**1** reveals the presence of another guest peak at 1.1 ppm overlapped with the capsule signals. The NOESY<sup>[17]</sup> and ROESY  $^1\text{H}$  NMR spectra (see Figure 2) confirm the presence of another signal at 1.1 ppm, which is in exchange with the signal at -0.3 ppm. The ROESY spectrum also shows exchange correlation signals between the signals at -1.5 and -3.1 ppm. Also, a series of 1D  $^1\text{H}$  NMR spectra were acquired at different temperatures (Figure 3). The peaks at -0.3, -1.5, and -3.1 ppm become broader with an increase in temperature and at 340 K they completely disappear. It was not possible to increase the temperature again because of the technical limits of the spectrometer, but probably the peaks at 1.1 and -0.3 ppm and the peaks at -1.5 and -3.1 ppm would coalesce into two signals. On the basis of the spectroscopic evidence collected, the assignment of the signals is that reported in Figure 1.

The value of  $\Delta G^{\ddagger}$  for rotation about the C–N bond for substrate **3** in mesitylene solution is 13.2 kcal mol<sup>-1</sup> versus 14.4 kcal mol<sup>-1</sup> inside **1**·**1** (see Table 1). The difference between the two barriers is 1.2 kcal mol<sup>-1</sup>, so the rotation is about eight times slower inside the capsule at room temperature. It is important to note that the coalescence tem-

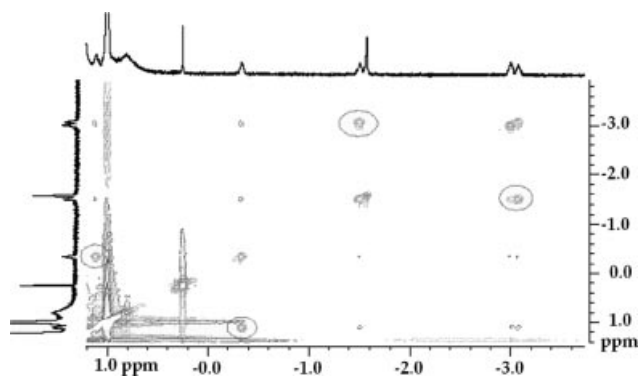


Figure 2. Upfield region of the ROESY spectrum of **3** encapsulated in **1**·**1**. The exchange spots are circled for clarity.

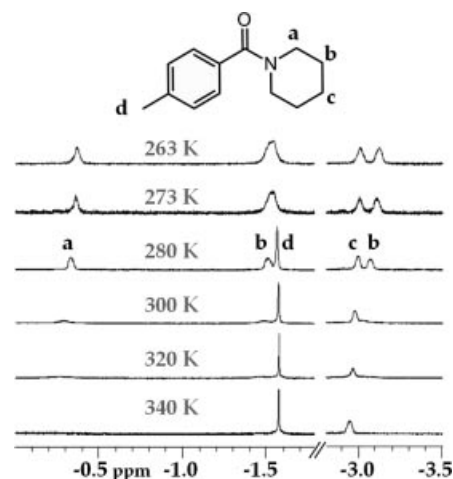


Figure 3. Upfield regions of the  $^1\text{H}$  NMR spectra of amide **3** encapsulated in **1**·**1** at different temperatures.

perature does not depend only on the barrier, but also on the chemical shift difference  $\Delta\nu$  of the signals at the slow exchange limit. The larger the value of  $\Delta\nu$ , the higher the coalescence temperature. In the case of guest **3**, the capsule has both an effect on the rotational rate and on  $\Delta\nu$  of the signals. The  $\Delta\nu$  values of the peaks in chemical exchange are larger in **1**·**1** than in solution.

We also studied acyclic guest **4**. Compound **4** was encapsulated and the exchange was found to be slow on the NMR timescale inside **1**·**1** and fast outside the capsule at room temperature. Methyl groups of this guest give two signals at -1.1 and -3.2 ppm and the methylene protons in the  $\alpha$  position show a signal at -0.15 ppm and another one overlapped with the capsule signals.<sup>[17]</sup> For compound **4**, the difference in the energy barrier of the encapsulated and free compound is about 1.4 kcal mol<sup>-1</sup> (Table 1). In this case, the rotation inside **1**·**1** is 10 times slower.

We studied amides similar to **3** but with different ring sizes, for example, compound **5**, which features a five-membered ring. The encapsulated compound shows a signal for one of the  $\alpha$  methylene protons at -0.4 ppm in exchange with another signal that overlaps with the capsule signals, and another two signals in chemical exchange at -2.0 and -2.7 ppm for the  $\beta$  methylene protons.<sup>[17]</sup> For amide **5**, the

barrier inside **1·1** is a little lower but the difference is only  $0.2 \text{ kcal mol}^{-1}$ , a difference comparable with the experimental error ( $\pm 0.2 \text{ kcal mol}^{-1}$ ).

In this case, we conclude that rotation about the C–N bond is about the same inside and outside the capsule; the cavity has no or little effect on this guest. In amides **6–8**, there is a methylene group between the carbonyl group and the aromatic ring. This structural variation affects the electronic properties of the amide but mostly the geometry and the flexibility of the compound. Amides **6** and **7** are very good guests and form very stable capsules in a wide range of temperatures. The upfield region of the  $^1\text{H}$  NMR spectrum of **6** encapsulated in **1·1** at 300 K looks very similar to the spectrum of encapsulated **3**.<sup>[17]</sup> We observed one signal at 0.0 ppm in chemical exchange with another signal further downfield but overlapped with other signals. The two methylene protons in the  $\beta$  position show two signals at  $-2.0$  and  $-3.0 \text{ ppm}$ .<sup>[17]</sup> These signals become broader as the temperature is increased and they completely disappear at 340 K. For this amide, the barrier of rotation inside the capsule is a little lower than outside. The value of  $\Delta\Delta G^{\circ\ddagger}$  between the two barriers is  $0.3 \text{ kcal mol}^{-1}$ , a small difference but bigger than the experimental error and probably meaningful. According to this difference in energy, compound **6** rotates nearly twice as fast inside **1·1** as it does in mesitylene solution at 300 K.

Amide **7** has a methyl group in the  $\gamma$  position of the piperidine ring. In this case, we observed two signals in chemical exchange at  $-2.2$  and  $-2.35 \text{ ppm}$  and another two signals in exchange at  $-2.7$  and  $-3.2 \text{ ppm}$ .<sup>[17]</sup> The first two signals in exchange are very close to each other and we observed two distinct signals at 280 K that became broader with an increase in the temperature. They coalesce at 315 K and a new signal at  $-2.25 \text{ ppm}$  appears. In this case, we observed slow exchange and coalescence, but fast exchange inside the capsule. For amide **7**, there is no meaningful difference between the barrier inside and outside the capsule (Table 1).

Amide **8**, which features two methyl groups in the  $\gamma$  position of the piperidine ring, was also studied to evaluate the effects of steric hindrance of the guest. The upfield regions of the  $^1\text{H}$  NMR spectra of **8** at different temperatures are reported in Figure 4. The only peaks in chemical exchange that do not overlap with other signals of the spectrum are at  $-2.0$  and  $-2.6 \text{ ppm}$ , which correspond to the methylene protons in the  $\beta$  position. As for **7**, we were able to see two distinct peaks in slow exchange at low temperature and just one peak at high temperature. It is remarkable that in this case, the barrier for the rotation of the guest is significantly lower inside than outside the capsule. The value of  $\Delta\Delta G^{\circ\ddagger}$  is  $-1.4 \text{ kcal mol}^{-1}$  (see Table 1), which corresponds to a rotation inside **1·1** that is about 11 times faster than in mesitylene solution. Here, the difference between the energy barriers is definitely much higher than the experimental error. Amide **9** is similar to guest **3**, but with a small structural change on the piperidine ring. It is not such a good guest because the capsule formed in the presence of this guest disassembles at temperatures lower than 290 K.<sup>[18]</sup> At

300 K, two very broad signals are visible and they become sharper as the temperature is increased.<sup>[17]</sup> These are the signals of the  $\alpha$  and  $\beta$  methylene protons. Therefore, in the case of amide **9**, it was not possible to measure the activation barrier because it was not possible to determine  $\Delta\nu$  at such a slow exchange limit.

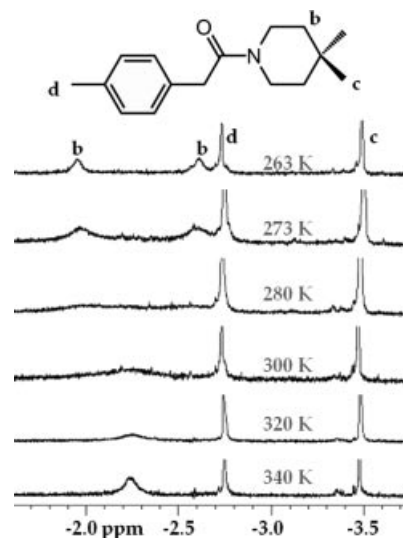


Figure 4. Upfield regions of the  $^1\text{H}$  NMR spectra of amide **8** encapsulated in **1·1** at different temperatures.

For the amides previously investigated, rotation about the C–N bond turns the molecule into another identical molecule (such as **3–6**, **8**, and **11**) or into its enantiomer (guests **7** and **9**). In these cases, the two ground states have the same stability. We also investigated the behavior of amide **10**, in which case the rotation about the C–N bond interconverts the two different isomers (Figure 5). The  $^1\text{H}$  NMR spectrum of **10** in deuterated mesitylene is very complicated because of the presence of two rotamers in rapid equilibrium. At 300 K, all of the protons signals on the piperidine ring are broadened. Decreasing the temperature to 273 K sharpens the signals and it is possible to integrate the signals of the methyl groups of the piperidine ring for the two isomers. The ratio of the two rotamers outside the capsule is, unsurprisingly, 1:1. Compound **10** is a very good guest for dimer **1·1**.

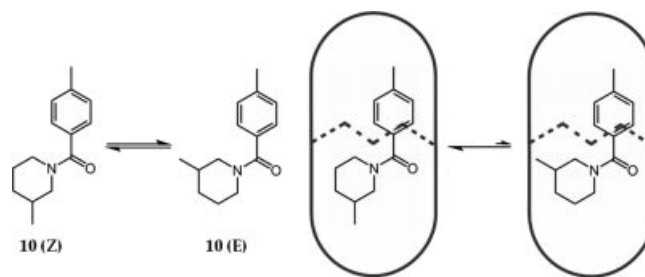


Figure 5. Equilibrium between the two isomers of amide **10** outside (left) and inside (right) the capsule.

The  $^1\text{H}$  NMR spectrum of guest **10** inside the capsule shows only one set of signals for the protons on the piperidine ring (see Figure 6). Furthermore, no change in the



spectrum is observed over a wide temperature range. Molecular modeling with *ab initio* calculations was carried out on amide **10** encapsulated in **1·1**.<sup>[17]</sup> The structure of this host–guest system shows that the most stable conformation of amide **10** is inside the capsule. It seems that the (*E*) conformation is unfavored because the methyl group on the piperidine ring clashes with the walls of the cavity. On the basis of this argument, it is reasonable to believe that the only conformation observed inside the capsule is the (*Z*) form (Figure 5). In the temperature range investigated, no signal corresponding to the (*E*) isomer was detected; consequently, it was not possible to give a quantitative estimate of the rotational barrier. Nevertheless, we can reasonably conclude that the rotation rate of **10** inside **1·1** is dramatically decreased.

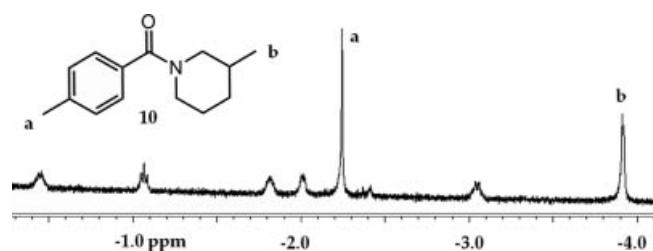


Figure 6. Upfield region of the  $^1\text{H}$  NMR spectrum of amide **10** at 273 K encapsulated in **1·1**.

The last compound, amide **11**, features a seven-membered ring and shows three sets of signals that undergo chemical exchange. Unfortunately, this compound was not a good guest for capsule **1·1**, and the proton spectra from 300 to 340 K show broad peaks and several coalescence phenomena.<sup>[17]</sup> It was not possible to assign the signals, even with the help of NOESY and ROESY spectra. They did not give any correlations for such broad peaks.

The only substrate that showed acceleration for the rotation about the C–N bond was amide **8**, the longest and the most sterically hindered at the extremity. The acceleration for guest **8** may be a destabilization of the ground state owing to the presence of two methyl groups on the piperidine ring. Computer models show that in amide **8**, one methyl clashes with the inner walls of the cavity, which causes steric repulsion.<sup>[17]</sup> To support this hypothesis, we carried out a competition experiment between amides **7** and **8**. Equimolar amounts of the two guests were dissolved in deuterated mesitylene (30 mM) in the presence of **1** (4 mM). Both compounds were encapsulated and by integration of the signals of the methyl groups on the piperidine ring inside the capsule it was possible to quantify their affinity for **1·1**.<sup>[17]</sup> The measured ratio for **7/8** was 8:1. This molar ratio corresponds to a difference of energy of about  $1.2 \text{ kcal mol}^{-1}$ . This value is very close to the difference of the activation energy  $\Delta\Delta G^\ddagger$  found for compound **8**. This experimental evidence suggests that **8** undergoes acceleration of the rotation inside the capsule because of ground-state destabilization.

## Conclusions

This research was undertaken to investigate the internal rotations of guests inside a nanoscale host. The energy barriers for the rotation about the C–N bond of several amides were measured by the coalescence method and compared with the barriers of the compounds free in solution. Several guests, differing in size and shape, were used. Amides **3** and **4** showed a decrease in their rotational rates, approximately 8 and 10 times slower, respectively. For guests **5–7**, the energy barriers inside and outside **1·1** are basically identical; the small differences observed are comparable with the experimental errors. Surprisingly, for amide **8**, the most sterically hindered guest, acceleration was observed (11 times faster) inside the capsule. A competition experiment between **7** and **8** showed a higher affinity of **7** for the capsule, which suggests that acceleration results from the destabilization of the ground state of the encapsulated guest. The rotation about the C–N bond in amide **10** generates two isomers that have a ratio of 1:1 when the compound is free in solution but inside dimer **1·1** only one rotamer was observed (see Figure 5). Accordingly, the rotation rate in the cavity is slowed by several orders of magnitude, if it occurs at all.

It is not easy to predict and rationalize these effects even *a posteriori*. Both attractive and repulsive forces take place inside the cavity. These forces can stabilize or destabilize the transition state of the rotation as well as the ground state. The inside of the capsule, mostly hydrophobic, has a polar region in the central belt of hydrogen bonds. The carbonyl group of the guests is very close to these N–H bonds, and it is known that the interaction of the carbonyl group of amides with Lewis acids results in an increase in the rotational barrier.<sup>[7]</sup> It is possible that such interactions contribute to the rotational barriers inside the capsule.

## Experimental Section

**Instruments and General Methods:** Anhydrous solvents and chemicals were obtained from Sigma–Aldrich or Acros Organics and used without any further purification. For the study of encapsulated guests and for the study of the rotational barriers of the free guests, 1D and 2D  $^1\text{H}$  NMR spectra were recorded at 600 MHz with a Bruker DRX-600. The other NMR spectra were recorded with a Varian 300 MHz.  $[\text{D}_{12}]$ Mesitylene was purchased from Cambridge Isotope Laboratories Inc. Andover, MA and was referenced to  $\delta_{\text{H}} = 2.11$  (Ar- $\text{CH}_3$ ) with respect to the resonance of  $(\text{CH}_3)_4\text{Si}$ . High resolution mass spectra were recorded with an Agilent ESI-TOF mass spectrometer.

**Materials:** Compound **1** was prepared according to the procedure described by Hayashida et al.<sup>[19]</sup> *N,N*-dimethylbenzamide (**2**) is commercially available (Aldrich, 99%), and it was used without any further purification. The other amides were synthesized according to the general procedure described below. All secondary amines used in the synthesis of guests **3–11** were commercially available except 4,4-dimethylpiperidine, which was synthesized according to a literature procedure.<sup>[20]</sup>

**General Procedure for the Synthesis of Amides 3–5 and 9–11:** To a solution of the secondary amine (12 mmol) in  $\text{CH}_2\text{Cl}_2$  (50 mL) was

added *p*-tolylacetylchloride (1.6 mL, 12 mmol) and triethylamine (3.4 mL, 24 mmol). The mixture was stirred overnight at room temp. and then diluted with CH<sub>2</sub>Cl<sub>2</sub> (50 mL), washed with NaOH (1 M; 20 mL), HCl (1 M; 20 mL), saturated NaHCO<sub>3</sub> (20 mL), and brine (20 mL). The organic phase was then dried with Na<sub>2</sub>SO<sub>4</sub>, filtered, and concentrated in vacuo. The crude residue was purified on silica gel.

**Piperidin-1-yl(*p*-tolyl)methanone (3):** Colorless oil. Yield: 1.851 g (76%). <sup>1</sup>H NMR (300 MHz, CDCl<sub>3</sub>): δ = 7.28 (d, *J* = 8.0 Hz, 2 H), 7.19 (d, *J* = 7.9 Hz, 2 H), 3.69 (m, 2 H), 3.36 (m, 2 H), 2.37 (s, 3 H), 1.67 (m, 2 H), 1.63 (m, 2 H), 1.53 (m, 2 H) ppm. <sup>13</sup>C NMR (75 MHz, CDCl<sub>3</sub>): δ = 170.5, 139.3, 133.5, 128.9, 126.9, 48.7, 43.1, 26.4, 25.7, 24.6, 21.3 ppm. HRMS (ESI-TOF): calcd. for C<sub>13</sub>H<sub>17</sub>NO [M + H]<sup>+</sup> 204.1383; found 204.1382.

***N,N*-Diethyl-2-naphthamide (4):** Colorless oil. Yield: 2.043 g (75%). <sup>1</sup>H NMR (300 MHz, CDCl<sub>3</sub>): δ = 7.89–7.80 (m, 4 H), 7.55–7.43 (m, 3 H), 3.43 (m, 4 H), 1.14 (m, 6 H) ppm. <sup>13</sup>C NMR (75 MHz, CDCl<sub>3</sub>): δ = 171.1, 134.4, 133.2, 132.6, 128.1, 127.6, 126.6, 126.4, 125.5, 123.7, 43.2, 39.2, 14.1, 12.8 ppm. HRMS (ESI-TOF): calcd. for C<sub>15</sub>H<sub>17</sub>NO [M + H]<sup>+</sup> 228.1383; found 228.1382.

**Pyrrolidin-1-yl(*p*-tolyl)methanone (5):** White solid. Yield: 2.086 g (92%). <sup>1</sup>H NMR (300 MHz, CDCl<sub>3</sub>): δ = 7.39 (d, *J* = 8.1 Hz, 2 H), 7.16 (d, *J* = 7.8 Hz, 2 H), 3.61 (m, 2 H), 3.41 (m, 2 H), 2.34 (s, 3 H), 2.00–1.76 (m, 4 H) ppm. <sup>13</sup>C NMR (75 MHz, CDCl<sub>3</sub>): δ = 169.7, 139.7, 134.2, 128.7, 127.1, 49.5, 46.1, 26.3, 24.3, 21.3 ppm. HRMS (ESI-TOF): calcd. for C<sub>12</sub>H<sub>15</sub>NO [M + H]<sup>+</sup> 190.1226; found 190.1225.

**(4-Methylpiperidin-1-yl)(*p*-tolyl)methanone (9):** Colorless oil. Yield: 1.770 g (68%). <sup>1</sup>H NMR (600 MHz, CDCl<sub>3</sub>): δ = 7.29 (d, *J* = 7.9 Hz, 2 H), 7.19 (d, *J* = 7.9 Hz, 2 H), 4.66 (m, 1 H), 3.75 (m, 1 H), 2.96 (m, 1 H), 2.76 (m, 1 H), 2.37 (s, 3 H), 1.74 (m, 1 H), 1.64 (m, 2 H), 1.17 (m, 2 H), 0.97 (d, *J* = 6.4 Hz, 3 H) ppm. <sup>13</sup>C NMR (150 MHz, CDCl<sub>3</sub>): δ = 170.4, 139.3, 133.5, 128.9, 126.9, 48.1, 42.5, 34.6, 33.8, 31.1, 21.7, 21.3 ppm. HRMS (ESI-TOF): calcd. for C<sub>14</sub>H<sub>19</sub>NO [M + H]<sup>+</sup> 218.1539; found 218.1539.

**(3-Methylpiperidin-1-yl)(*p*-tolyl)methanone (10):** Colorless oil. Yield: 2.109 g (81%). <sup>1</sup>H NMR (600 MHz, CDCl<sub>3</sub>): δ = 7.30 (d, *J* = 7.9 Hz, 2 H), 7.21 (d, *J* = 8.2 Hz, 2 H), 4.54 (m, 1 H), 3.72 (m, 1 H), 2.89 (m, 1 H), 2.54 (m, 1 H), 2.39 (s, 3 H), 1.87 (m, 1 H), 1.68 (m, 2 H), 1.53 (m, 1 H), 1.18 (m, 1 H), 0.91 (m, 3 H) ppm. <sup>13</sup>C NMR (150 MHz, CDCl<sub>3</sub>): δ = 170.4, 139.3, 133.5, 128.9, 126.9, 55.1 (br.), 48.3 (br.), 42.7 (br.), 33.1, 31.3 (br.), 25.2 (br.), 21.3, 18.9 ppm. HRMS (ESI-TOF): calcd. for C<sub>14</sub>H<sub>19</sub>NO [M + H]<sup>+</sup> 218.1539; found 218.1540.

**Azepan-1-yl(*p*-tolyl)methanone (11):** Colorless oil. Yield: 2.0 g (77%). <sup>1</sup>H NMR (600 MHz, CDCl<sub>3</sub>): δ = 7.26 (d, *J* = 8.0 Hz, 2 H), 7.18 (d, *J* = 7.7 Hz, 2 H), 3.66 (m, 2 H), 3.37 (m, 2 H), 2.36 (s, 3 H), 1.83 (m, 2 H), 1.66–1.55 (m, 6 H) ppm. <sup>13</sup>C NMR (150 MHz, CDCl<sub>3</sub>): δ = 171.6, 138.9, 134.4, 128.9, 126.5, 49.7, 46.3, 29.5, 27.8, 27.2, 26.4, 21.3 ppm. HRMS (ESI-TOF): calcd. for C<sub>14</sub>H<sub>19</sub>NO [M + H]<sup>+</sup> 218.1539; found 218.1536.

**General Procedure for the Synthesis of Amides 6–8:** To a solution of *p*-tolylacetic acid (2 g, 13 mmol) in CH<sub>2</sub>Cl<sub>2</sub> (50 mL) was added the secondary amine (14 mmol), triethylamine (3.7 mL, 26 mmol), and PyBroP (6.5 g, 14 mmol). The mixture was stirred overnight at room temp. and then diluted with CH<sub>2</sub>Cl<sub>2</sub> (50 mL), washed with NaOH (1 M; 20 mL), HCl (1 M; 20 mL), satd. NaHCO<sub>3</sub> (20 mL), and brine (20 mL). The organic phase was then dried with Na<sub>2</sub>SO<sub>4</sub>, filtered, and concentrated in vacuo. The crude residue was purified on silica gel.

**1-(Piperidin-1-yl)-2-*p*-tolylethanone (6):** Colorless oil. Yield: 2.143 g (76%). <sup>1</sup>H NMR (300 MHz, CDCl<sub>3</sub>): δ = 7.15 (m, 4 H), 3.71 (s, 2 H), 3.59 (m, 2 H), 3.38 (m, 2 H), 2.34 (m, 3 H), 1.56 (m, 4 H), 1.37 (m, 2 H) ppm. <sup>13</sup>C NMR (75 MHz, CDCl<sub>3</sub>): δ = 169.0, 135.6, 131.9, 128.9, 128.0, 46.8, 42.4, 40.3, 25.8, 25.1, 24.0, 20.6 ppm. HRMS (ESI-TOF): calcd. for C<sub>14</sub>H<sub>19</sub>NO [M + H]<sup>+</sup> 218.1539; found 218.1539.

**1-(4-Methylpiperidin-1-yl)-2-*p*-tolylethanone (7):** Colorless oil. Yield: 2.538 g (85%). <sup>1</sup>H NMR (300 MHz, CDCl<sub>3</sub>): δ = 7.11 (m, 4 H), 4.58 (m, 1 H), 3.81 (m, 1 H), 3.67 (s, 2 H), 2.90 (m, 1 H), 2.53 (m, 1 H), 2.31 (s, 3 H), 1.68–1.50 (m, 3 H), 1.15–0.75 (m, 2 H), 0.88 (d, *J* = 6.2 Hz, 3 H) ppm. <sup>13</sup>C NMR (75 MHz, CDCl<sub>3</sub>): δ = 169.4, 136.0, 132.2, 129.2, 128.3, 46.4, 42.1, 40.7, 34.3, 33.6, 30.9, 21.6, 20.9 ppm. HRMS (ESI-TOF): calcd. for C<sub>15</sub>H<sub>21</sub>NO [M + H]<sup>+</sup> 232.1696; found 232.1696.

**1-(4,4-Dimethylpiperidin-1-yl)-2-*p*-tolylethanone (8):** Colorless oil. Yield: 2.229 g (70%). <sup>1</sup>H NMR (300 MHz, CDCl<sub>3</sub>): δ = 7.11 (m, 4 H), 3.67 (s, 2 H), 3.56 (m, 2 H), 3.34 (m, 2 H), 2.31 (m, 3 H), 1.31 (m, 2 H), 1.16 (m, 2 H), 0.91 (s, 6 H) ppm. <sup>13</sup>C NMR (75 MHz, CDCl<sub>3</sub>): δ = 169.4, 136.0, 132.2, 129.2, 128.3, 42.8, 40.6, 38.7, 38.3, 37.9, 28.9, 27.6, 20.9 ppm. HRMS (ESI-TOF): calcd. for C<sub>16</sub>H<sub>23</sub>NO [M + H]<sup>+</sup> 246.1852; found 246.1855.

**Study of the Rotational Barriers:** To prepare the sample for the study of the encapsulated amides, a deuterated mesitylene solution (450 μL) of **1** (4 mM) and the guest (30 mM) was prepared and sonicated overnight. To obtain a good signal-to-noise ratio, 250 scans were acquired for each <sup>1</sup>H NMR spectrum. For the measurement of the rotational barriers outside the capsule, a sample (450 μL) of a deuterated mesitylene solution of the guest (30 mM) was used. In the competition experiment between **7** and **8**, the two guests were dissolved in mesitylene in the same concentration (30 mM) and then 4 mM of **1** was added. The sample was used after sonication overnight.

**Supporting Information** (see footnote on the first page of this article): Various spectral data for compound **2–9** and **11** and the computer structures of **8** and **10** encapsulated in **1·1**.

## Acknowledgments

We are grateful to the Skaggs Foundation and the National Institutes of Health (GM 50174) for support. We thank Prof. C. L. Perrin for advice and fruitful discussion, and acknowledge Dr. D.-H. Huang and Dr. L. Pasternack for NMR assistance.

- [1] a) T. Heinz, D. M. Rudkevich, J. Rebek Jr, *Nature* **1998**, *394*, 764–766; b) A. Scarso, L. Trembleau, J. Rebek Jr, *Angew. Chem. Int. Ed.* **2003**, *42*, 5499–5502; c) T. Amaya, J. Rebek Jr, *J. Am. Chem. Soc.* **2004**, *126*, 14149–14156; d) J. Rebek Jr, *Angew. Chem. Int. Ed.* **2005**, *44*, 2068–2078; e) T. Iwasawa, D. Ajami, J. Rebek Jr, *Org. Lett.* **2006**, *8*, 2925–2928; f) A. R. Albulnia, C. Gaeta, P. Neri, A. Grassi, G. Milano, *J. Phys. Chem. B* **2006**, *110*, 19207–19214; g) T. Heinz, D. M. Rudkevich, J. Rebek Jr, *Angew. Chem. Int. Ed.* **1999**, *38*, 1136–1139.
- [2] A. Scarso, H. Onagi, J. Rebek Jr, *J. Am. Chem. Soc.* **2004**, *126*, 12728–12729.
- [3] R. G. Chapman, J. C. Sherman, *J. Am. Chem. Soc.* **1995**, *117*, 9081–9082.
- [4] a) B. M. O’Leary, R. M. Grotzfeld, J. Rebek Jr, *J. Am. Chem. Soc.* **1997**, *119*, 11701–11702; b) R. Grotzfeld, N. Branda, J. Rebek Jr, *Science* **1996**, *271*, 487–489.
- [5] W. E. Stewart, T. H. Siddall, *Chem. Rev.* **1970**, *70*, 517–551.
- [6] For some recent studies, see: a) Y. Otani, O. Nagae, Y. Naruse, S. Inagaki, M. Ohno, K. Yamaguchi, G. Yamamoto, M. Uchi-

- yama, T. Ohwada, *J. Am. Chem. Soc.* **2003**, *125*, 15191–15199; b) E. D. Glendenning, J. A. Hrabal, *J. Am. Chem. Soc.* **1997**, *119*, 12940–12946; c) D. Lauvergnat, P. C. Hiberty, *J. Am. Chem. Soc.* **1997**, *119*, 9478–9482.
- [7] a) G. Fraenkel, C. Franconi, *J. Am. Chem. Soc.* **1960**, *82*, 4478–4483; b) T. Drakenberg, K. I. Dahlqvist, S. Forsén, *J. Phys. Chem.* **1972**, *76*, 2178–2183; c) A. J. Bennet, V. Somayaji, R. S. Brown, B. D. Santarsiero, *J. Am. Chem. Soc.* **1991**, *113*, 7563–7571; d) C. Cox, D. Ferraris, N. N. Murthy, T. Lectka, *J. Am. Chem. Soc.* **1996**, *118*, 5332–5333; e) C. Cox, T. Lectka, *J. Org. Chem.* **1998**, *63*, 2426–2427.
- [8] J. C. Sherman, C. B. Knobler, D. J. Cram, *J. Am. Chem. Soc.* **1991**, *113*, 2194–2204.
- [9] a) G. D. Van Duyne, R. F. Standaert, P. A. Karplus, S. L. Schreiber, J. Clardy, *J. Mol. Biol.* **1993**, *229*, 105–124; b) J. Fanghänel, *Angew. Chem. Int. Ed.* **2003**, *42*, 490–492.
- [10] a) G. Fischer, *Angew. Chem. Int. Ed. Engl.* **1994**, *33*, 1415–1436; b) S. C. R. Lummis, D. L. Beene, L. W. Lee, H. A. Lester, R. W. Broadhurst, D. A. Dougherty, *Nature* **2005**, *438*, 248–252.
- [11] G. Fischer, *Biomed. Biochim. Acta* **1984**, *43*, 1101–1111.
- [12] a) G. Fischer, *Chem. Soc. Rev.* **2000**, *29*, 119–127; b) E. S. Eberhardt, *J. Am. Chem. Soc.* **1992**, *114*, 5437–5439.
- [13] S. Mecozzi, J. Rebek Jr, *Chem. Eur. J.* **1998**, *4*, 1016–1022.
- [14] K. T. Chapman, W. C. Still, *J. Am. Chem. Soc.* **1989**, *111*, 3075–3077.
- [15] A. Allerhand, H. S. Gutowsky, J. Jonas, R. A. Meinzer, *J. Am. Chem. Soc.* **1966**, *88*, 3185–3194.
- [16] M. L. Martin, F. Mabon, M. Trierweller, *J. Phys. Chem.* **1981**, *85*, 76–78.
- [17] See Supporting Information.
- [18] T. Amaya, J. Rebek Jr, *J. Am. Chem. Soc.* **2004**, *126*, 14149–14156.
- [19] O. Hayashida, L. Sebo, J. Rebek Jr, *J. Org. Chem.* **2002**, *67*, 8291–8298.
- [20] T. Hayashi, M. Sawamura, Y. Ito, *Tetrahedron* **1992**, *48*, 1999–2012.

Received: February 23, 2007  
Published Online: April 17, 2007